JOURNAL OF COMPUTATIONAL PHYSICS 111, 282–290 (1994)

Decoupling Approximations Applied to an Infinite Array of Fluid Loaded Baffled Membranes*

C. L. SCANDRETT

Department of Mathematics, Naval Postgraduate School, Monterey, California 93940

AND

G. A. KRIEGSMANN

Department of Mathematics and the Center for Applied Mathematics and Statistics, New Jersey Institute of Technology, Newark, New Jersey

Received June 19, 1992; revised October 7, 1993

Application of a time-dependent nonlocal radiation boundary condition, used in conjunction with the finite difference technique, is applied to the acoustic problem of scattering from an infinite array of baffled, fluid-loaded membranes. The new boundary operator is compared with the second-order Engquist and Majda boundary operator and with several fluid/structure decoupling approximation techniques in the determination of scattering amplitudes.

INTRODUCTION

The scattering of a plane acoustic wave by a periodic array of baffled membranes is studied in this paper. This scattering problem is not only mathematically and physically interesting in its own right, but it is also a critical component for an analysis of a large finite array [1, 2]. In the paper by Crighton *et al.* [3], the example of scattering from an array of fluid-loaded membranes is reviewed as a simple model which displays many of the features found in scattering from more complicated arrays, such as scattering and radiation from transducer arrays [4] and periodically stiffened plates used in hull construction [5]. This paper addresses the numerical problem of solving such scattering problems and explores the usefulness of recent approximate techniques.

Floquet theory is first applied to reduce the physical domain above the array into a fundamental cell which is a waveguide-like region above a single membrane. The solution in this cell is composed of propagating and evanescent modes which carry the scattered energy away from the membrane. Next, a new radiation boundary operator is derived which essentially annihilates all the propagating modes when applied at an artificial boundary $y = R_b$, which is several wavelengths above the array. Using this operator and finite differences provides an accurate numerical approximation to the scattered field in the truncated fundamental cell.

In addition to developing an accurate finite difference scheme to study the scattering problem, three approximate methods are proposed and implemented. The first two are derived from a pseudo-differential equation formulation of the problem wherein the back pressure from a single membrane is expressed as the square root of a differential operator. Approximations relating the membrane displacement to the pressure are obtained by approximating the square root by its truncated Taylor series or a rational function. Using the first term in the Taylor series gives the plane wave approximation [6] while using the first two terms gives an approximation derived elsewhere by Kriegsmann and Scandrett, and Miksis and Ting (KSMT) [7–9] for a single baffled membrane. Both these approximations yield simple analytical results for the field within the fundamental cell. Finally, the third approximation comes about by truncating the Green's function to incorporate only the propagating modes of the cell. Then the integro-differential equation for the membrane motion is solved using finite differences. This is called the propagating mode approximation (PM) or NLRB (nonlocal radiation boundary condition) approximation.

Results using these three aprproximations are compared against those of the full finite difference scheme (FFD). Except for frequencies near resonance, the plane wave and KSMT approximations agree very well with the FFD results—the KSMT approximation being slightly superior. Near resonant frequencies the plane wave approximation becomes inaccurate while the KSMT approximation is still quite good. In both cases the PM approximation gives

* Supported by O.N.R. Contract Number N00014-92-J-1261.

0021-9991/94 $6.00

excellent results although it requires considerably more numerical effort.

An outline of the paper follows. In Section 1, the formulation of the problem is given; followed by Section 2, which gives a description of the finite difference scheme and the radiation operator. In this section, comparison of the new operator to the second-order radiation operator of Engquist and Majda [10] is done. Section 3 outlines the derivation of the approximate techniques used, and the paper concludes with several examples.

1. FORMULATION

A periodic array of identical membranes, each of length A, is held in place by an acoustically rigid infinite baffle. The uniform spacing between membranes is B, resulting in a periodic geometry of period $2a$, where $2a = A + B$. Above the array is a homogeneous and isotropic acoustic fluid and below it a vacuum. The baffled structure is insonified by a plane time harmonic pressure wave of radial frequency ω (see Fig. 1a).

In dimensionless variables $\mathbf{x} = (x, y)$, the equation governing the pressure in the fluid is

$$\nabla^2 P + k^2 P = 0, \tag{1}$$

where $k = \omega A/c_a$ and c_a is the sound speed in the fluid. The spatial variables were made dimensionless by scaling with respect to A.

The equation for the lateral displacement of the jth membrane after scaling is

$$\frac{d^2 W_j}{dx^2} + c^2 k^2 W_j = \varepsilon c^2 k^2 P((x, 0; k), \qquad x \in \Omega_j, \quad |j| = 1, 2, ..., \infty, \tag{2}$$

where the dimensionless parameters c and ε are ratios of fluid to membrane wave speeds (c_a/c_m) and densities $(\rho_a A/\rho_m)$, respectively. The Ω_j denote the set of points occupied by the jth membrane. The ratio of pressure to membrane displacement scale factors is $A\omega^2\rho_a$.

The presence of the acoustically hard baffle introduces the boundary condition

$$\frac{\partial P}{\partial y}(x, 0) = 0, \qquad x \notin \Omega, \tag{3a}$$

where Ω is that portion of the plane occupied by the baffles, while fixing the membranes' endpoints on the baffle requires

$$W_j = 0, \qquad x \in \partial\Omega_j, \qquad |j| = 1, 2, ..., \infty, \tag{3b}$$

where $\partial\Omega_j$ denotes the end points of the jth membrane. Equating the time harmonic normal velocities of the fluid and membrane at their points of contact yields

$$\frac{\partial P}{\partial y} = W_j, \qquad x \in \Omega_j, \quad y = 0. \tag{4}$$

The plane incident time harmonic pressure P^I is a solution of (1) and is given by

$$P^I(x, y; k) = \tfrac{1}{2} e^{-ik(x\cos\Theta_I + y\sin\Theta_I)}, \tag{5}$$

where Θ_I is the angle that the incident wave makes with the positive x axis and the time dependence is assumed to be $e^{-i\omega t}$. If the line $y = 0$ were entirely rigid, then the incident wave would be reflected as $P^I(x, -y, k)$. Accordingly, the total pressure is decomposed as

$$P(x, y; k) = P^I(x, y; k) + P^I(x, -y; k) + p(x, y; k), \qquad 0 < y, \tag{6}$$

where the effect of the periodic array is manifest in p, the scattered field.

Inserting (6) into (1)–(4) it is found that p satisfies

$$\nabla^2 p + k^2 p = 0, \qquad 0 < y, \tag{7a}$$

$$\frac{\partial p}{\partial y} = \begin{cases} 0, & x \in \bar{\Omega} \\ W_j, & x \in \Omega_j \end{cases} \tag{7b}$$

$$\frac{d^2 W_j}{dx^2} + c^2 k^2 W_j = \varepsilon c^2 k^2 \{2P^I(x, 0; k) + p(x, 0; k)\}, \qquad x \in \Omega_j \tag{7c}$$

$$W_j = 0, \qquad x \in \partial\Omega. \tag{7d}$$

The formulation of the scattering problem is completed by requiring p to behave as an outgoing wave at ∞.

The formal solution of (7a) is given by

$$p(x, y; k) = \sum_{-\infty}^{\infty} a_n e^{i\gamma_n x + i\beta_n y}, \qquad y > 0 \tag{8a}$$

$$\beta_n = \sqrt{k^2 - \gamma_n^2} \tag{8b}$$

$$\gamma_n = -k\cos\Theta_I + n\pi/a, \tag{8c}$$

where the reflection coefficients a_n are to be determined. This solution is formally valid for all (x, y) above the baffled membranes. The numbers β_n in (8b) are the propagation constants of the reflected waves scattered by the surface. For given k, Θ_I, and a, there are only a finite number of these that are purely real. That is, there are numbers $N(k, \Theta_I, a)$ and $M(k, \Theta_I, a)$ such that β is real for $-M \leqslant j \leqslant N$ and is purely imaginary for $j > N$ and $j < -M$. The latter modes represent surface waves which decay exponentially for $y > 0$,

while the former correspond to radiating waves. Finally, using conservation of flux (or power) arguments it is readily found that the coefficients a_n, for the propagating waves, satisfy the relationship

$$\Im \int_{-1/2}^{1/2} \bar{p} W_0(x)\, dx = 2a \sum_{-M}^{N} \beta_n \|a_n\|^2, \tag{9}$$

where the overbar denotes complex conjugation and the $\Im$, the imaginary part of a complex number.

2. FINITE DIFFERENCE SCHEME

The finite difference scheme which is used to solve the coupled fluid structure problem is very similar to that presented in Kriegsmann and Scandrett [7]. It is an explicit time marching scheme which is second-order accurate in both time and space. The solution of the time harmonic problem is obtained from the explicit time domain calculations as a result of the limiting amplitude principle [11], which guarantees the approach to a steady state.

The spatial domain used is: $|x| \leqslant a$ and $0 \leqslant y \leqslant R_b$. Unlike the single baffled membrane problem, wherein a radiation boundary condition needed to be applied in the fluid surrounding the membrane, the periodic array requires a radiation boundary condition only at $y = R_b$. (Along $x = \pm a$, periodic boundary conditions are required.) In order for the radiation boundary condition to successfully model the infinite fluid, it must prevent reflection of the *radiating* modes generated by the fluid/membrane interaction.

Because the number of existing radiating modes and their directions of propagation are dependent upon the incident angle (Θ_I), frequency (k) of the insonifying plane wave, and a separation parameter (a), the radiation boundary condition applied at R_b must be flexible. Incorporated into the finite difference code is a time dependent nonlocal radiation boundary condition which effectively inhibits reflections from the boundary of all radiating modes. The radiation condition is similar to that used in the work of Fix and Marin [12], except that it is applied in the time domain rather than the frequency domain.

Development of the radiation condition follows from the time harmonic form of Eq. (8a). For large values of y, evanescent modes are neglected and the scattered pressure is

$$p(x, y, t; k) \approx \sum_{n=-M}^{N} a_n e^{i\gamma_n x + i\beta_n y - it}. \tag{10}$$

A radiation boundary condition which annihilates the nth propagating mode is

$$B_n(\phi) = \frac{\partial \phi}{\partial y} + \beta_n \frac{\partial \phi}{\partial t}. \tag{11}$$

Applying boundary operators to each of the several modes yields

$$\sum_{n=-M}^{n} B_n\{a_n(t)\, e^{i\gamma_n x + i\beta_n y}\} \approx 0, \tag{12}$$

where the time dependence of the modes has been incorporated into the coefficients a_n. The time dependent coefficients $a_n(t)$ can be found from the time-dependent form of Eq. (8a) as

$$a_n(t) = \frac{1}{2a} \int_{-a}^{a} e^{-i(\beta_n y + \gamma_n \xi)} p(\xi, y, t)\, d\xi. \tag{13}$$

Inserting (13) into (12), applying (11), taking the partial with respect to y outside of the summation, and writing explicitly the $a_n(t)$ coefficient in the summation yields the boundary operator:

$$\frac{\partial p}{\partial y} \approx -\frac{1}{2a} \sum_{n=-M}^{N} \beta_n \int_{-a}^{a} e^{i\gamma_n (x-\xi)} \frac{\partial p}{\partial t}(\xi, y, t)\, d\xi. \tag{14}$$

The above boundary operator is then center differenced and combined with the center-differenced form of the wave equation resulting in a matrix equation for the unknown values of the pressure at the artificial boundary, $y = R_b$.

While application of the boundary operator does require a matrix factorization requiring $O(n^3)$ operations, the factorization need be done only once *before* the advent of time domain difference calculations. Subsequent solutions of the unknown pressures at the artificial boundary are found using the *factored* form of the matrix which requires only $O(n^2)$ operations and, therefore, is relatively quick.

A stopping criterion is applied to halt the calculations when solutions to the problem at two different times differ by less than a prescribed tolerance level. In all of the results given, the iterations were stopped when the integrated membrane displacement *and* the integrated pressure at the artificial boundary differed in successive time levels by less than 0.00005.

A comparison was made with the current radiation boundary condition and the second-order Engquist and Majda boundary operator [10, Eq. (9)]. The Engquist and Majda operator was finite-differenced in time and space, combined with the discretized form of the wave equation and periodic boundary conditions leading to a circulent Jacobi matrix, which is in turn solved repeatedly (as is NLRB) for the values of the unknown pressures at the artificial boundary of the numerical domain. Physically, this operator was designed to handle scattering problems for which the scattered wave should strike the artificial boundary at near normal incidence (a condition not always met in waveguides). A more appropriate boundary operator

for waveguides is derived in Kriegsmann [13], but it becomes cumbersome if more than two modes of the waveguide are propagating. For this reason, the Engquist and Majda operator was chosen for the comparison. The two methods were tested on a waveguide problem for which analytical solutions were known. In particular, the waveguide was forced at one end ($x=0$) by known

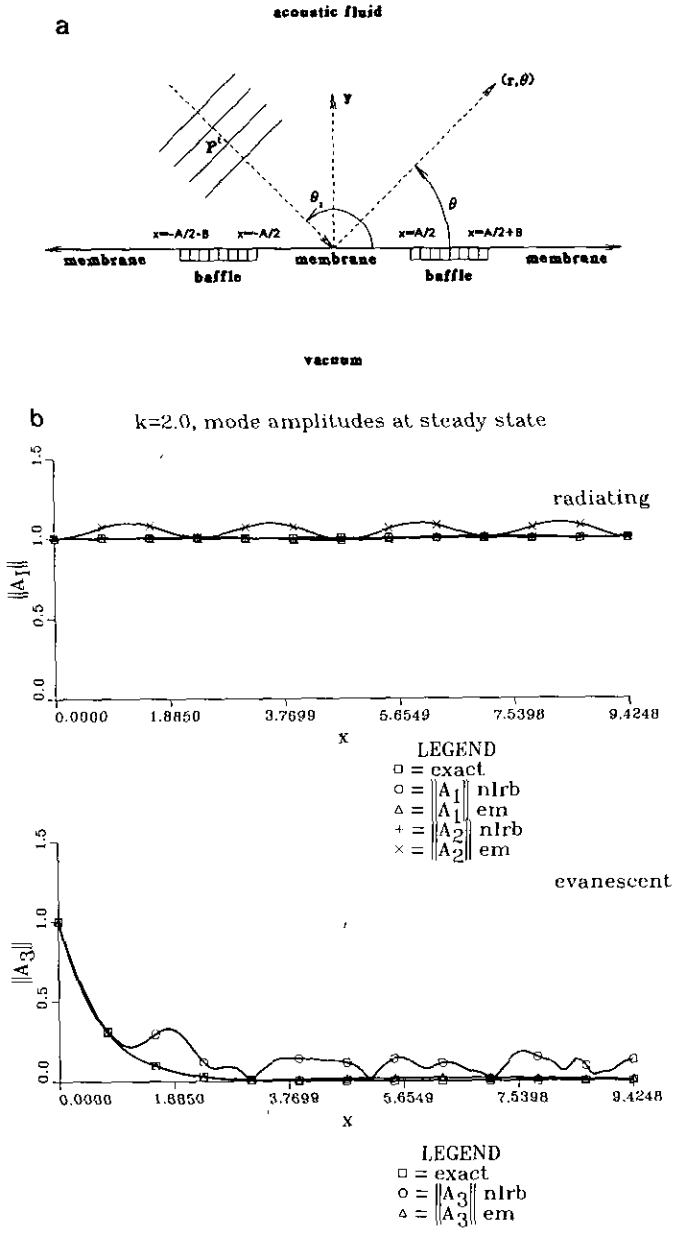

FIG. 1. (a) Problem configuration. (b) Comparison of the nonlocal (NLRB) and Engquist and Majda (EM) radiation boundary operators. Boundary conditions for the waveguide are homogeneous Dirichlet ($y=\pi$) and homogeneous Neumann ($y=0$), resulting in two propagating modes. Amplitudes of the two propagating and one of the evanescent modes are plotted as a function of the position along the waveguide (x). The exact answer should be one for each propagating mode and exponentially decreasing for the evanescent mode.

propagating and evanescent modes. The side boundary conditions for this example were homogeneous Dirichlet at $y=\pi$ and homogeneous Neumann at $y=0$. Exciting the first three modes:

$$u_n = \cos(s_n y)\, e^{ix\sqrt{k^2-s_n^2}-it}, \qquad s_n = \frac{2n-1}{2}, \qquad n = 1, 2, \ldots,$$

with amplitudes of one and running the finite difference codes which were identical, except in their radiation boundary condition for 4000 iterations produced the mode amplitudes as functions of x shown in Fig. 1b. As can be seen, the Engquist and Majda operator does significantly better with the evanescent modes than does the nonlocal radiation condition. However, in determining the amplitudes of the propagation modes, the Engquist and Majda operator produces an unwanted standing wave pattern. This type of pattern is less noticeable with the first mode compared to the second, due to the fact that the first mode's direction of propagation is more nearly normal to the artificial boundary, and therefore the Engquist and Majda boundary operator introduces only a negligible reflection. For this simple problem, it is possible to analytically calculate the amplitude of the standing wave pattern. Doing so for the second propagating mode at $x=3\pi/8$ the theoretical value is found to be 1.085 while the numerical solution yields 1.094. The incident angle of the second propagating mode measured from the boundary normal is $\tan^{-1}(s_2/\beta_2) \approx 48.6°$. For problems in which incident angles are in excess of this value, amplitudes of the standing wave patterns get considerably larger. It is also true that the amplitude of the standing wave is a function of where the artificial boundary has been placed and upon which mode and what value of k has been used.

For the fluid membrane coupled problem, it is difficult to know where to "best" determine the amplitudes of the propagating modes if one uses the Engquist and Majda radiation condition. One must also be concerned with spurious evanescent waves in applying the nonlocal boundary operator. For these reasons, both boundary conditions are used and compared. The results presented in the sequel demonstrate that the nonlocal boundary operator gives membrane displacement shapes very similar to those using the Engquist and Majda boundary operator. Furthermore, in cases where there is a significant amount of radiated energy, the nonlocal boundary operator more nearly satisfies the energy conservation condition (Eq. (9)).

It should be noted that the Engquist and Majda radiation condition produces a matrix-type operator just as the nonlocal boundary operator method does. In problems where Neumann, Dirichlet, or mixed B.C. are imposed on the sides of the waveguide, the Engquist and Majda operator is tridiagonal in a form which is, of course, easier to handle than the full complex matrix produced by the nonlocal radiation

condition. However, for periodic boundary conditions, the matrix for the Engquist and Majda condition remains sparse, but it is no longer tridiagonal.

3. APPROXIMATE TECHNIQUES

In this section three approximations relating $p(x, 0)$ to $(\partial p/\partial y)(x, 0)$ are given. Two of these are derived from the Kriegsmann and Scandrett [9] method, while the third is a result of applying the time harmonic version of the radiation boundary operator (Eq. (14)) on the surface of the membrane.

When the Kriegsmann and Scandrett approximation for a single membrane is inserted into (7c) an equation for $W_j(x)$ alone is obtained. From (8a)

$$\frac{\partial p}{\partial y}(x, 0) = \sum_{-\infty}^{\infty} A_n e^{i\gamma_n x} \tag{15a}$$

$$p(x, 0) = -i \sum_{-\infty}^{\infty} \frac{A_n}{\beta_n} e^{i\gamma_n x}, \tag{15b}$$

where $A_n = i\beta_n a_n$. By expanding $1/\beta_n$ in a power series in terms of γ_n/k, inserting this expansion into (15b), interchanging the orders of summation, formally replacing terms of the form $\gamma_n^{2m} e^{i\gamma_n x}$ by $(-1)^m (d^{2m}/dx^{2m}) e^{i\gamma_n x}$, resumming the infinite series, and using (10a) Eq. (15b) becomes

$$p(x, 0) = -\frac{i}{k} \frac{1}{\sqrt{1 + D^2/k^2}} \frac{\partial p}{\partial y}(x, 0), \tag{16}$$

where $D = d/dx$. Inserting (16) into (7c) and using (7b) gives the pseudo-differential equation

$$\frac{d^2 W_j}{dx^2} + c^2 k^2 W_j = = \varepsilon c^2 k^2 \left\{ 2P^I(x, 0; k) - \frac{i}{k} \frac{1}{\sqrt{1 + D^2/k^2}} W_j(x) \right\}, \quad x \in \Omega_j. \tag{17}$$

Pseudo-differential equations involving square roots of differential operators occur in other branches of wave propagation and, in particular, underwater acoustics [14]. There, theories such as the parabolic approximation and the wide angle parabolic approximation arise by replacing the square root by a polynomial or a rational function in the differential operator. In an analogous fashion an approximate differential equation for the displacement of the jth membrane is deduced from (17) by approximating $1/\sqrt{1 + D^2/k^2}$ by a polynomial in D^2/k^2. For example, if only the first term of its Taylor series is used, then

$$\frac{d^2 W_j}{dx^2} + c^2 k^2 \left[1 + \frac{i\varepsilon}{k} \right] W_j = 2\varepsilon c^2 k^2 P^I(x, 0; k), \qquad x \in \Omega_j. \tag{18}$$

This is just the "plane wave approximation," because the same approximation gives

$$p(x, 0) = -\frac{i}{k} \frac{\partial p}{\partial y}(x, 0) = -\frac{i}{k} W_j(x). \tag{19}$$

A more useful and accurate approximation results when the first two terms of the Taylor series are used. Then, the approximate equation becomes

$$\left[1 - \frac{i\varepsilon c^2}{2k} \right] \frac{d^2 W_j}{dx^2} + c^2 k^2 \left[1 + \frac{i\varepsilon}{k} \right] W_j = 2\varepsilon c^2 k^2 P^I(x, 0; k), \qquad x \in \Omega_j, \tag{20}$$

and the corresponding result for $p(x, 0)$ is

$$p(x, 0) = -\frac{i}{k} \left[1 - \frac{D^2}{2k^2} \right] W_j(x). \tag{21}$$

These are the same expressions derived in Kriegsmann and Scandrett [7] for a single membrane and Miksis and Ting [8] for a single membrane under a different limiting process.

The third approximation for the surface pressure in terms of the membrane displacement is found in the following manner. Set Eq. (15a) equal to W_j and the coefficient a_n $(= A_n/i\beta_n)$ can be found in terms of the jth membrane's displacement:

$$a_n = \frac{1}{2ia\beta_n} \int_{-1/2}^{1/2} e^{-i\gamma\xi} W_j(\xi)\, d\xi. \tag{22}$$

Upon substitution of Eq. (22) into Eq. (15b) and neglecting evanescent modes, one obtains the third approximation used in this paper,

$$p(x, 0) = -\frac{i}{2a} \sum_{n=-M}^{N} \frac{1}{\beta_n} \int_{-1/2}^{1/2} W_j(\xi)\, e^{i\gamma_n(x-\xi)} d\xi. \tag{23}$$

This final approximation yields an integro-differential equation for the jth membrane displacement and is therefore nearly as hard to solve as the fully coupled problem, except that the number of modes has been reduced from infinite to only those which involve radiation of energy from the surface.

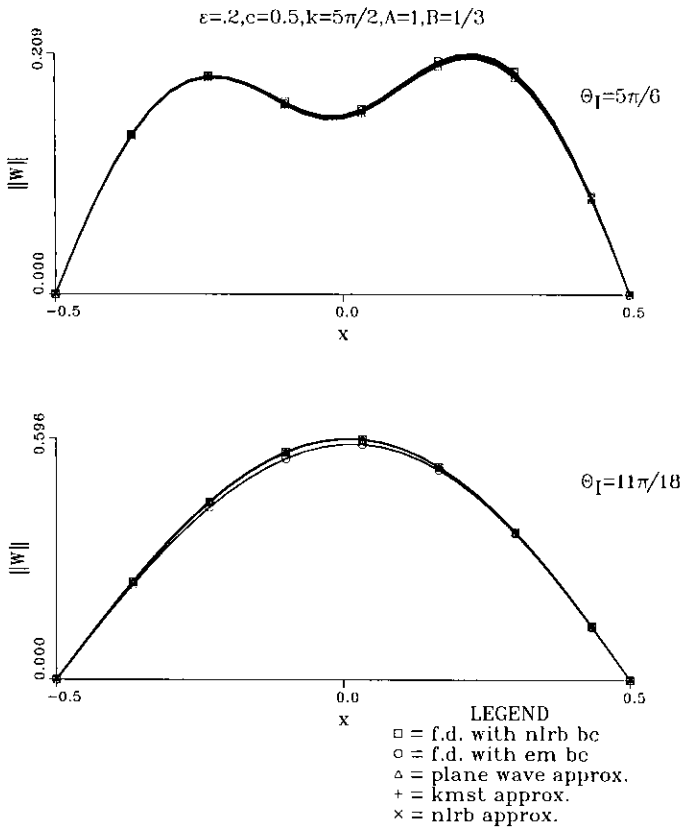

FIG. 2. Comparison of solutions displaying membrane displacement at a nonresonant (*in vacuo*) frequcency for two different incident angles.

4. NUMERICAL RESULTS

A series of graphs will be presented to show the applicability of the three impedance approximations, as well as some confirmation of the finite difference scheme used. In each of the examples, the following values are fixed: $c = 0.5$, $\varepsilon = 0.2$, $A = 1.0$, $\Delta x = \frac{1}{30}$ (except for the final figure for which it is $\frac{1}{50}$), and $\Delta t = 0.9k\,\Delta x/\sqrt{1 + 1/c^2}$. The three parameters k, B, and Θ_I are varied to determine their effect on the solution of the scattering problem.

In Fig. 2a plane wave of frequency other than an *in vacuo* eigenfrequency strikes the array at two different angles. In each case, it would appear that all of the approximate methods give results equivalent to the finite difference solutions. For the case $\Theta_I = 11\pi/18$ four radiating plane waves are excited (i.e., β_n is real for $-2 \leqslant n \leqslant 1$), while for $\Theta_I = 5\pi/6$ the four radiating plane waves are associated with β_n, where $-3 \leqslant n \leqslant 0$. In each case the modal coefficients a_n, found using the values of the membrane displacement (whose magnitudes are plotted in Fig. 2), are given in Table I and can be seen to be in excellent agreement. For this example, the conservation equation (9) is nearly satisfied by both of the finite difference solutions. The relative error in trying to satisfy Eq. (9) is given by

$$R = \frac{\Im \int_{-1/2}^{1/2} \bar{p} W_0(x)\,dx - 2a \sum_{-M}^{N} \beta_n \|a_n\|^2}{\Im \int_{-1/2}^{1/2} \bar{p} W_0(x)\,dx}. \quad (24)$$

For the cases $\Theta_I = 5\pi/6$ and $\Theta_I = 11\pi/18$, the values of R were NLRB: -0.0715 (0.0039), EM (Engquist and Majda boundary condition): -0.0076 (0.0041); and NLRB: -0.0253 (0.0253), EM: 0.0607 (0.0265), respectively. The values in parenthesis are the numerical values of the imaginary part of the integrals. In subsequent discussion, the values of R and of the imaginary parts of the corresponding integrals are given in Table III.

In Figs. 3 and 4, the frequency associated with $k = 2\pi$ corresponds to the first *in vacuo* eigenfrequency of the membranes. In Fig. 3 two plots are shown in which the value of Θ_I is different while Fig. 4 shows the effect of varying the spacing between membranes. In both figures the third approximation matches very well with the finite difference calculation, whereas the PWA and KSMT approximations are off. The relative errors made at the point of maximum deflection of the membrane are approximately 7%, 5%,

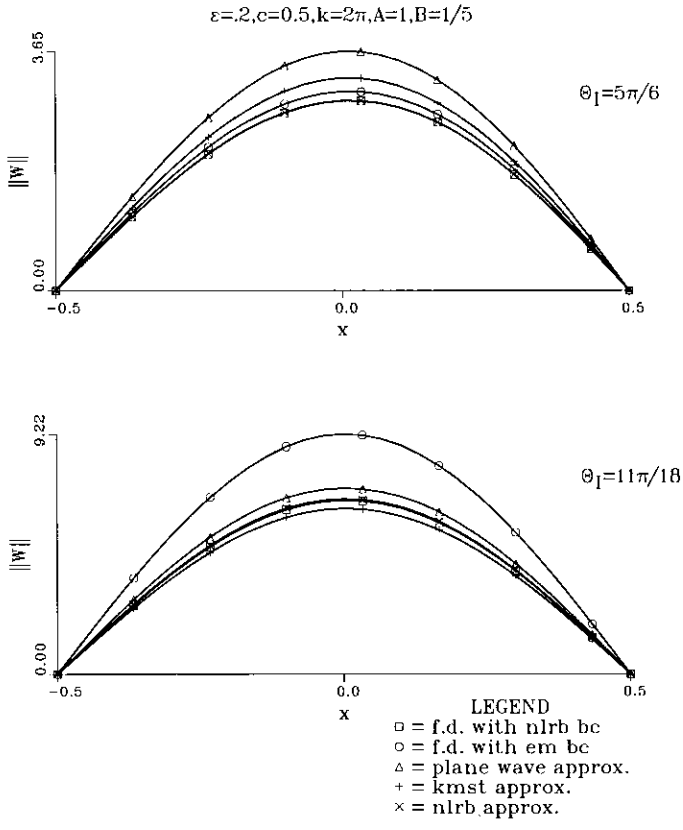

FIG. 3. Same as Fig. 2 except that the membranes are being excited at their first *in vacuo* resonant frequency, again for two different incident angles.

TABLE I

a_n	FD	PWA	KMST	NLRB	a_n	FD	PWA	KMST	NLRB
				Figure 2					
		$\Theta_I = 5\pi/6$					$\Theta_I = 11\pi/18$		
a_{-2}	0.02812	0.02795	0.02794	0.02792	a_{-3}	0.01614	0.01590	0.01590	0.01597
a_{-1}	0.03704	0.03670	0.03668	0.03662	a_{-2}	0.01506	0.01485	0.01484	0.01488
a_0	0.02860	0.02827	0.02826	0.02818	a_{-1}	0.00738	0.00727	0.00727	0.00727
a_1	0.00928	0.00906	0.00908	0.00901	a_0	0.00843	0.00828	0.00829	0.00837
				Figure 4					
		$B = 2/3$					$B = 1$		
a_{-3}	0.19058	0.24477	0.21755	0.19280	a_{-3}	0.14007	0.16089	0.14299	0.14160
a_{-2}	0.16436	0.21172	0.18818	0.16666	a_{-2}	0.15914	0.18336	0.16299	0.16131
a_{-1}	0.16686	0.21526	0.19135	0.16941	a_{-1}	0.15140	0.17493	0.15551	0.15381
a_0	0.15726	0.20317	0.18068	0.15989	a_0	0.14597	0.16931	0.15057	0.14876
				Figure 5					
		$\Theta_I = 2\pi/3$					$\Theta_I = 2.01\pi/3$		
a_{-3}	Cutoff	Cutoff	Cutoff	Cutoff	a_{-3}	0.59231	0.80478	0.71529	0.60270
a_{-2}	0.12081	0.28866	0.25657	0.29394	a_{-2}	0.21231	0.28689	0.25500	0.21480
a_{-1}	0.13465	0.31802	0.28268	0.32375	a_{-1}	0.23438	0.31512	0.28010	0.23598
a_0	0.12317	0.28871	0.25665	0.29383	a_0	0.21363	0.28523	0.25356	0.21369

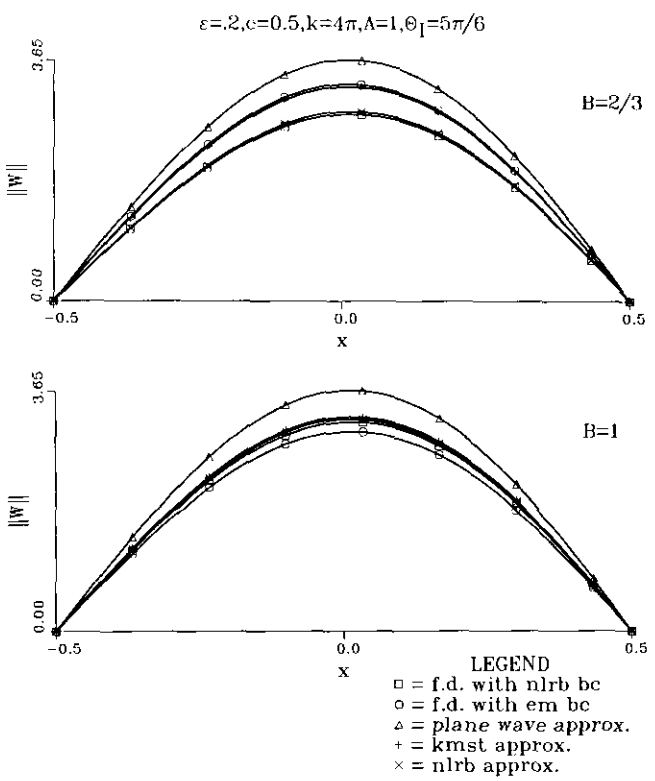

FIG. 4. Same as Fig. 3, except that results are displayed at the first *in vacuo* resonant frequency of the membranes for two different intermembrane spacings.

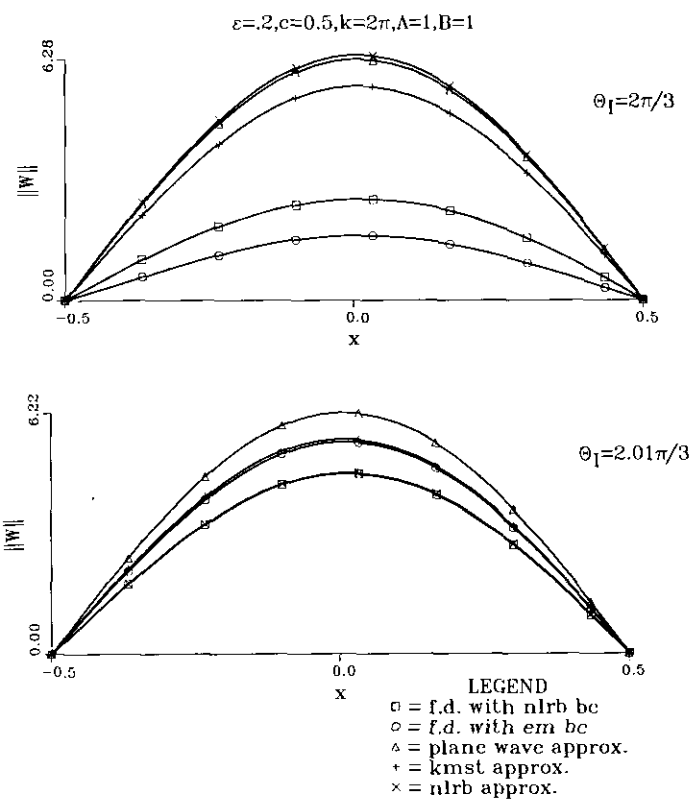

FIG. 5. Comparison of solutions at and near the waveguide cutoff frequency. Cutoff occurs at $\Theta_I = 2\pi/3$.

and $<1\%$ for the PWA, KSMT, and NLRB approximations, respectively, with $\Theta_I = 11\pi/18$. The relative errors increase for $\Theta = 5\pi/6$, where again the PWA approximation is worst, while the NLRB approximation is best with a relative error $<1\%$. In comparing the finite difference codes employing the values of R given from the table, one might assume that the nonlocal boundary operator is doing much better than the Engquist and Majda operator. The worst case for the latter operator being Fig. 3 with $\Theta_I = 11\pi/18$ with an R value of 0.44 compared to 0.0041 for the nonlocal operator. A possible explanation for the large value of R in the Engquist and Majda solution is that the pressure and membrane displacement are incorrectly phased at the fluid membrane interface, causing some error in calculating the pressure-displacement integral.

Because the PWA and KSMT approximations derived in Sections 3 are the same as those presented in Kriegsmann and Scandrett [9] for a single baffled membrane, one might expect that these approximations are unable to account for interactions between membranes. Figure 4 shows the results of varying the value of B and, in fact, the KSMT and PWA solutions are found to be identical. One would conclude

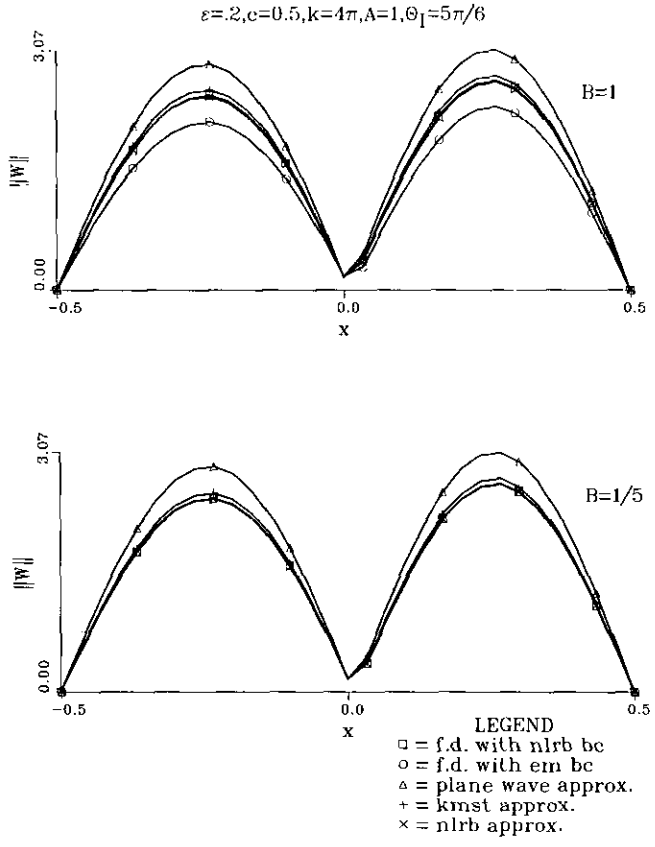

FIG. 6. Comparison of solutions showing membrane displacement at the second *in vacuo* resonant frequency of the membranes for two different inter-membrane spacings.

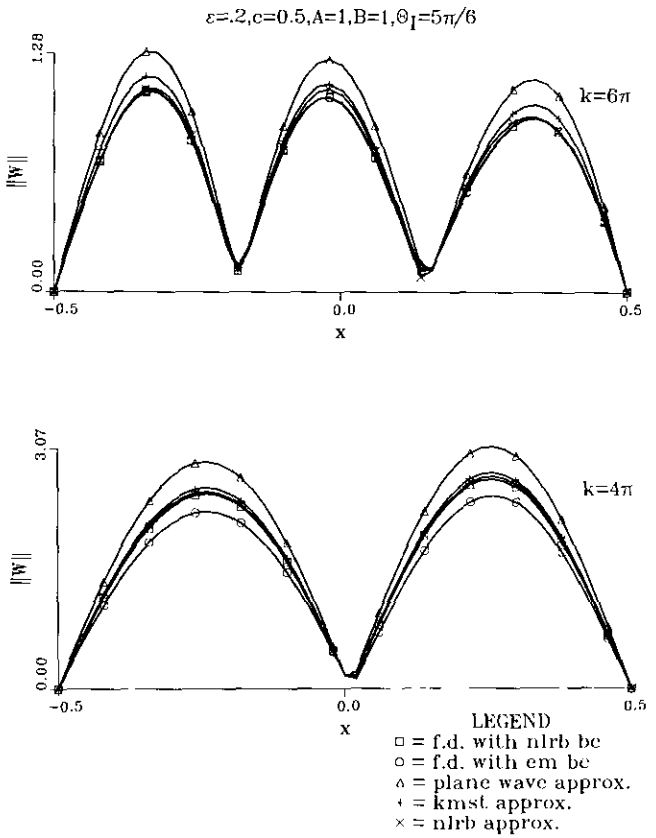

FIG. 7. Comparison of solutions showing membrane displacement at the second and third *in vacuo* resonant frequencies of the membranes.

that these approximations are therefore of limited value in problems where interactions between membranes are presumed to be strong.

Figure 5 is included to show what happens at "cutoff," which occurs when one of the β_i equals zero. At this frequency it is hard to assess which, if any, of the methods is doing a good job. For this case the finite difference code using the Engquist and Majda operator is presumably the "best" since it has a lower R value than the nonlocal finite difference solution. Its R value is still, however, relatively high (0.2543). For the case just above cutoff, it can be seen that none of the approximate methods do very well nor does the finite difference code with the Engquist and Majda operator. The reason for their failure lies in the fact that a significant amount of energy is being radiated away at an angle of $\approx 82°$ from the normal to the boundary (see the amplitude of A_{-3} in the tables). Just as the Engquist and Majda require near normal incidence to eliminate unwanted reflections, so too can the PWA and KSMT approximations be thought of as valid for cases of near normal scattering from the radiating membranes.

Figure 6 is similar to Fig. 4 in that the spacing between membranes is allowed to vary, while holding Θ_I and k fixed.

TABLE II

a_n	FD	PWA	KMST	NLRB	a_n	FD	PWA	KMST	NLRB
				Figure 7					
		$k=6\pi$					$k=4\pi$		
a_{-11}	0.00732	0.00947	0.00843	0.00785	a_{-11}	NR	NR	NR	NR
a_{-10}	0.00212	0.00223	0.00199	0.00191	a_{-11}	NR	NR	NR	NR
a_{-9}	0.01160	0.01392	0.01238	0.01161	a_{-9}	NR	NR	NR	NR
a_{-8}	0.01535	0.01856	0.01651	0.01544	a_{-8}	NR	NR	NR	NR
a_{-7}	0.00884	0.01069	0.00951	0.00887	a_{-7}	0.02188	0.02544	0.02262	0.02236
a_{-6}	0.00185	0.00226	0.00201	0.00192	a_{-6}	0.05165	0.06004	0.05337	0.05257
a_{-5}	0.00539	0.00652	0.00580	0.00546	a_{-5}	0.05716	0.06642	0.05904	0.05808
a_{-4}	0.00206	0.00252	0.00225	0.00214	a_{-4}	0.02637	0.03062	0.02722	0.02672
a_{-3}	0.01244	0.01505	0.01338	0.01280	a_{-3}	0.02301	0.02673	0.02376	0.02336
a_{-2}	0.01512	0.01819	0.01618	0.01580	a_{-2}	0.05622	0.06522	0.05798	0.05682
a_{-1}	0.00879	0.01022	0.00923	0.00964	a_{-1}	0.05352	0.06190	0.05507	0.05375
a_0	0.00556	0.00568	0.00560	0.00526	a_0	0.02570	0.02922	0.02621	0.02522

The *second in vacuo* eigenfrequency of the membrane is at $k=4\pi$. It is shown in Fig. 6 that, in fact, the difference in spacing between membranes has very little effect on the acutal membrane displacement. It does, however, affect which and how many modes will radiate energy. For $B=1$, there are eight radiating plane waves $-7\leqslant n\leqslant 0$, while for $B=\frac{2}{3}$ there are only five, $-4\leqslant n\leqslant 0$.

The final figure compares the results of exciting the membranes at their second and third *in vacuo* eigenfrequencies with separation and incident angle fixed. At higher frequencies, it can be seen that the KSMT approximation does a "better" job in mimicking the correct membrane displacement and hence the coefficients of the radiated plane waves. All approximations can be shown to approach the PWA for large frequencies since in that limit the $\beta_n \to k$, and Eqs. (21) and (23) collapse to Eq. (19). Results for the computed coefficients can be found in Table II.

TABLE III

Case	R(NLRB)	∫(NLRB)	R(EM)	∫(EM)
		Figure 2		
$\Theta_I=5\pi/6$	−0.0715	0.0039	−0.0076	0.0041
$\Theta_I=11\pi/18$	−0.0253	0.0253	0.0607	0.0265
		Figure 3		
$\Theta_I=5\pi/6$	−0.0011	0.8417	−0.0510	0.8830
$\Theta_I=11\pi/18$	0.0041	3.780	−0.4429	4.973
		Figure 4		
$B=2/3$	0.0093	0.8207	−0.1646	0.9391
$B=1$	0.0121	0.9191	0.0549	0.8726
		Figure 5		
$\Theta_I=2\pi/3$	0.5559	1.242	0.2543	0.2851
$\Theta_I=2.01\pi/3$	−0.0001	2.269	−0.2281	2.573
		Figure 6		
$B=1$	0.0105	0.3096	0.1313	0.2670
$B=1/5$	0.0163	0.3093	0.0122	0.3090
		Figure 7		
$k=6\pi$	0.0168	0.0325	0.0058	0.0322
$k=4\pi$	0.0050	0.3043	0.0883	0.2778

REFERENCES

1. A. K. Jordan and R. H. Lang, *Radio Sci.* **14**, 1077 (1979).
2. G. A. Kriegsmann, *J. Acoust. Soc. Am.* **88**, 492 (1990).
3. D. G. Crighton and D. Innes, *J. Sound Vib.* **91**, 293 (1983).
4. A. C. Hennion, R. Bossut, J. N. Decarpigny, C. Audoly, *J. Acoust. Soc. Am.* **87**, 1861 (1990).
5. C. H. Hodges, J. Power, and J. Woodhouse, *J. Sound Vib.* **101**, 219 (1985).
6. R. D. Mindlin and H. H. Bleich, *J. Appl. Mech.* **20**, 189 (1953).
7. G. A. Kriegsmann and C. L. Scandrett, *J. Acoust. Soc. Am.* **86**, 788 (1989).
8. M. J. Miksis and L. Ting, *Wave Motion* **11**, 545 (1989).
9. G. A. Kriegsmann and C. L. Scandrett, *Appl. Math. Lett.* **3**, 51 (1990).
10. R. Clayton and B. Engquist, *Bull. Seismol. Soc. Am.* **67**, 1529 (1977).
11. C. S. Morawetz, *Commun. Pure Appl. Math.* **15**, 349 (1962).
12. G. J. Fix and S. P. Marin, *J. Comput. Phys.* **28**, 253 (1978).
13. G. A. Kriegsmann, *SIAM J. Sci. Stat. Comput.* **3**, 318 (1982).
14. F. D. Tappert, in *Wave Propagation and Underwater Acoustics*, Lecture Notes in Physics, Vol. 70, edited J. Keller and J. S. Papadakis (Springer-Verlag, New York/Berlin, 1977), p. 224.